Provided for non-commercial research and education use.
Not for reproduction, distribution or commercial use.

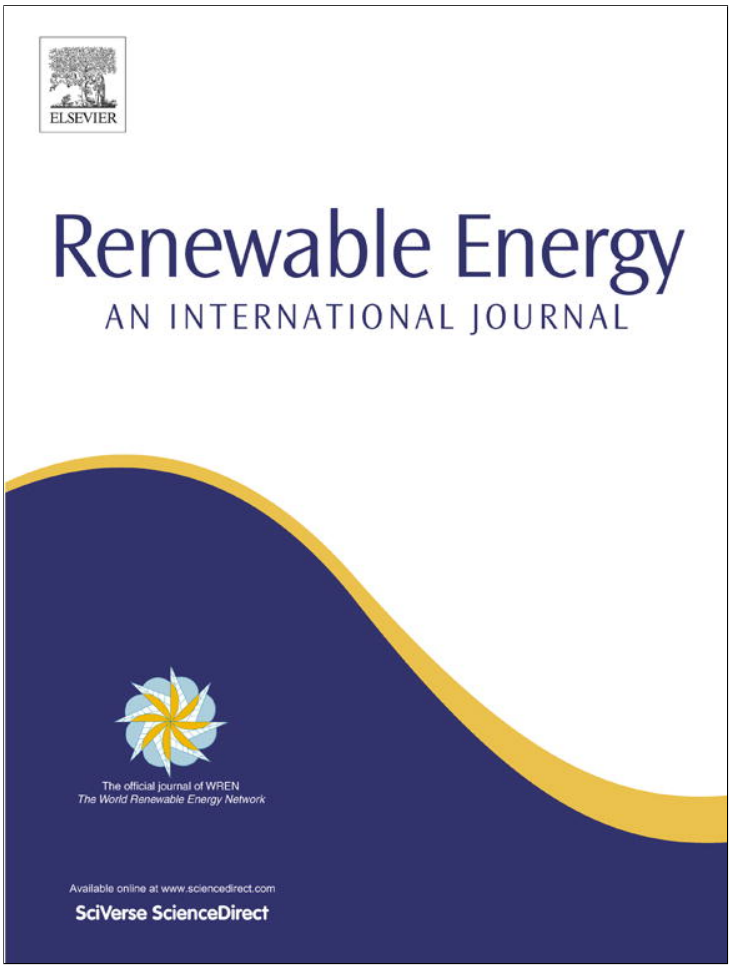

(This is a sample cover image for this issue. The actual cover is not yet available at this time.)

This article appeared in a journal published by Elsevier. The attached copy is furnished to the author for internal non-commercial research and education use, including for instruction at the authors institution and sharing with colleagues.

Other uses, including reproduction and distribution, or selling or licensing copies, or posting to personal, institutional or third party websites are prohibited.

In most cases authors are permitted to post their version of the article (e.g. in Word or Tex form) to their personal website or institutional repository. Authors requiring further information regarding Elsevier's archiving and manuscript policies are encouraged to visit:

http://www.elsevier.com/copyright

Author's personal copy

Renewable Energy 57 (2013) 422–431

Contents lists available at SciVerse ScienceDirect

Renewable Energy

journal homepage: www.elsevier.com/locate/renene

Effects of mooring systems on the performance of a wave activated body energy converter

Barbara Zanuttigh [a,*], Elisa Angelelli [a], Jens Peter Kofoed [b]

[a] University of Bologna, DICAM, Viale Risorgimento 2, 40136 Bologna, Italy
[b] Aalborg University, Dep. of Civil Engineering, Sohngårdsholmsvej 57, 9000 Aalborg, Denmark

ARTICLE INFO

Article history:
Received 16 July 2012
Accepted 7 February 2013
Available online

Keywords:
Wave energy converters
Power production
Wave transmission
Mooring system
Wave obliquity
Experiments

ABSTRACT

Aim of this paper is to analyse the power and hydraulic performance of a floating Wave Energy Converter with the purpose at optimising its design for installation in arrays. The paper presents new experiments carried out in 1:30 scale on a single device of the Wave Activated Body type in the deep-water wave tank at Aalborg University. Power production and wave transmission were examined by changing the mooring system, the wave attack and the device orientation with respect to the incoming waves.. To assure the best performance the device size may be "tuned" based on the local peak wave length and the mooring system should be selected to allow the device for large movements.

© 2013 Elsevier Ltd. All rights reserved.

1. Introduction

For optimising power capture, Wave Energy Converters (WECs) must operate at or near resonance. Therefore moorings of WECs should allow for large motions of the structure, in order to serve their primary function, but also comply with many other requirements [1], for example interact with the body dynamic in order to increase the overall efficiency. So far there is very limited research dedicated to verify to which extent the mooring arrangements are influencing the hydrodynamic loading on the structure, as well as the power extraction capabilities [2].

Floating WECs (f-WECs), specifically suited to severe wave conditions, reduce by absorption the incident wave energy and may thus be used not only for energy production but also for coastal protection purposes. Also the research devoted to the changes of the wave field around f-WECs is fairly limited. A detailed experimental study on a single f-WEC, a model of the Wave Dragon (www.wavedragon.net), was performed by Nørgaard and Pulsen, [3]. However, the knowledge gained from floating breakwaters (FB) can provide a substantial contribution to define the wave transmission coefficient K_T for f-WECs. For FBs, K_T is often given as a function of peak wave period T_p and significant wave height H_s, the FB geometrical and dynamic properties (mass, added mass, damping factor, natural period of oscillation) and finally of the characteristics of the mooring system [4,5]. K_T is usually related to l/L_p, being L_p the peak wave length and l the FB length parallel to the incident wave direction. The larger the incident wave length L_p relatively to l, the larger the K_T [6]. It is therefore expected that a sufficiently long f-WEC may be effective in reducing wave transmission.

Aim of this contribution is to examine both the power production and hydraulic performance of a given f-WEC, i.e. DEXA device (www.dexawave.com), depending on the mooring system. DEXA is an f-WEC that belongs to the Wave Activated Body (WAB) type, where the energy production is based on the relative movement of separate parts.

Preliminary tests showed that for high values of the wave steepness DEXA is very effective [7], and therefore may produce energy also when the sea conditions are not extreme, such as in case of strong winds in short fetches.

In order to assess if DEXA is suitable solution for installation in a multi-purpose wave farm, the specific objective of this paper is to analyse how the device efficiency η and the transmission coefficient K_T vary with mooring type, wave height, wave steepness and orientation of the device with respect to incoming waves.

Section 2 describes the tests, including the facility, the device geometry, the mooring system, the tested regular and irregular wave conditions and the performed measurements. Section 3 specifically addresses the process adopted for optimising the

* Corresponding author.
E-mail addresses: barbara.zanuttigh@unibo.it (B. Zanuttigh), elisa.angelelli4@unibo.it (E. Angelelli), tla@civil.aau.dk (J.P. Kofoed).

0960-1481/$ – see front matter © 2013 Elsevier Ltd. All rights reserved.
http://dx.doi.org/10.1016/j.renene.2013.02.006

Author's personal copy

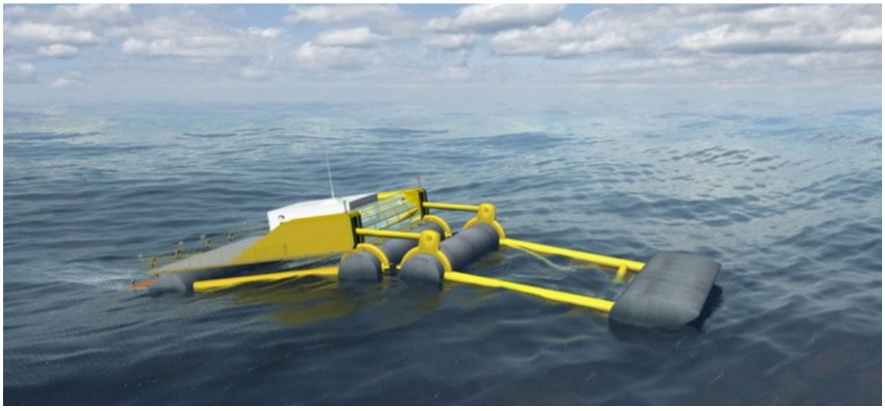

Fig. 1. 3D rendering image showing a single DEXA device full scale (from www.dexawave.com).

rigidity of the Power Take-Off (PTO) system in order to maximise power production and device efficiency. Section 4 describes the wave field around the device in terms of wave transmission, wave reflection, wave radiation and changes of wave direction induced by the device. The design and performance of such installation based on the joint analysis of the dependence of η and K_T on l/L_p are also discussed. Some conclusions are finally drawn in Section 5.

2. Description of the tests

2.1. The facility

The hydrodynamic tests were performed in the deep-water directional wave basin of the Hydraulics and Coastal Engineering Laboratory at Aalborg University, DK. The basin is 15.7 m long (waves direction), 8.5 m wide and 1.5 m deep. The wave generator is a snake-front piston type composed of 10 actuators with maximum stroke length of 0.5 m, enabling generation of short-crested waves. The software used for controlling the paddle system is AwaSys developed by the same laboratory [8]. Regular and irregular long and short crested waves with peak periods up to approximately 2.5 s, oblique 2D and 3D waves can be generated with good results.

Passive wave absorption is carried out. A 1:4 dissipative beach made of concrete and gravel with average diameter $D_{50} = 5$ cm is placed opposite to the wave maker. The sidewalls are made of crates (1.21 $\times$ 1.21 m, 0.70 m deep).

2.2. The device

The DEXA device consists of two rigid pontoons with a hinge in between, which allows each pontoon to pivot in relation to the other (Fig. 1). The draft is such that at rest the free water surface passes in correspondence of the axis of the four buoyant cylinders. The Power Take-Off (PTO) system consists of a low pressure power transmission technology based on water ("Aquagear") and is placed close to the centre of the system, in order to maximise the stabilisation force [7].

In the laboratory, one DEXA model (Fig. 2) was adopted in scale 1:30. The model is 2.10 m long cross-shore and 0.81 m wide long-shore, and totally weighs 33 kg, the weight of the PTO system being about 10 kg.

The device brings on board a PTO system (Fig. 3) that consists of a metal bar with an elongate-shaped hole, a wire welded at the two ends of the hole and a small electric engine with a wheel. The bar is connected to one half of the device and the wheel to the other, via a load cell (strain gauge equipped "bone"). The wire is rolled up around the wheel that is forced to rotate while translating along the bar hole. The rigidity of the PTO was modified by varying the resistance of the wheel to rotation and therefore the current in the engine. It was possible to set up to 17 rigidities.

Two mooring systems were tested (Fig. 4). One is the up-scaled reproduction of the "spread type" [1]. It consists of four steel chains which are fixed to the bottom with heavy anchors and are linked to the device at the fairlead point in the middle of the legs by

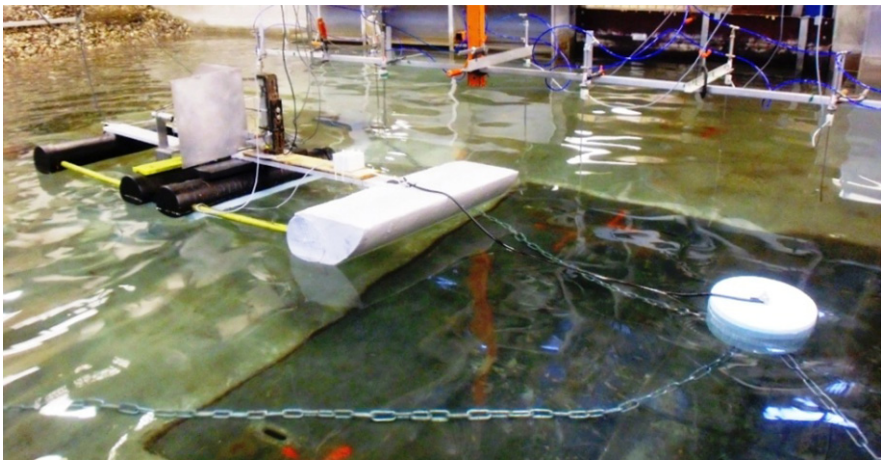

Fig. 2. Picture of the DEXA model, 1:30 scale, in the deep water wave basin, Aalborg, DK. CALM mooring system.

Author's personal copy

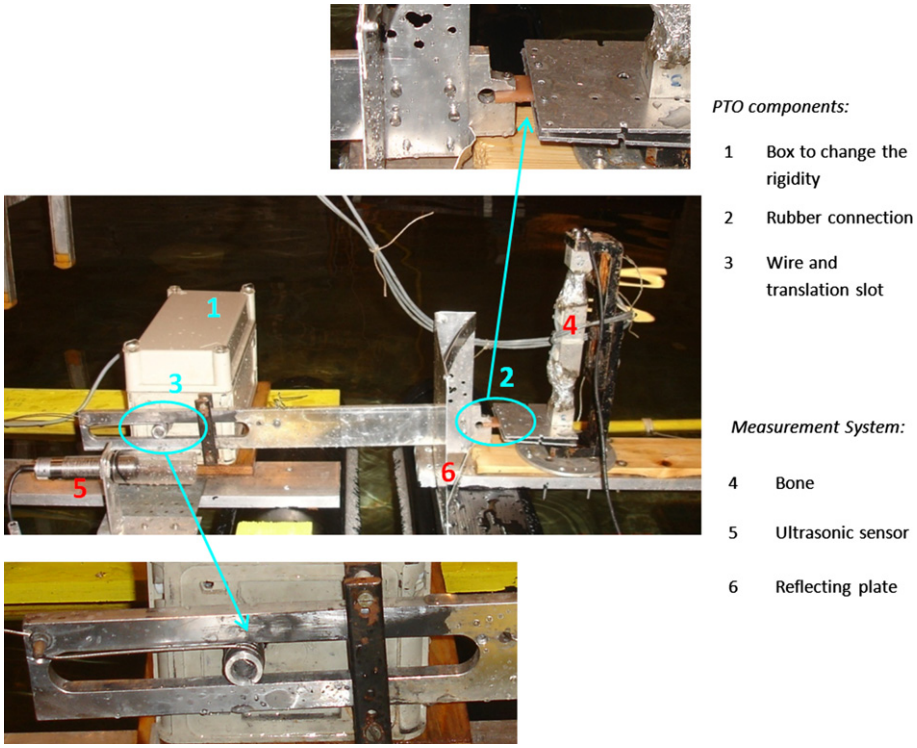

Fig. 3. Zoomed view of the PTO system.

means of a resistant plastic strip. The other type is the "catenary anchor leg mooring" (CALM) system (Harris et al., 2004) where the device is linked to a buoy moored with four chains and it is able to rotate around it according to the prevailing wave direction. In both systems the chains were characterised by 3.0 m length and 1.0 kg/m and the 4 anchors were 30 kg heavy. Chains were designed based on the catenary equations [9], the length of the chain portion raised from the bottom being about 1/3 of the total chain length. In the CALM system, the cylindrical polystyrene buoy, whose diameter was 0.28 m, was linked to the device through a 1.30 m long elastic cable.

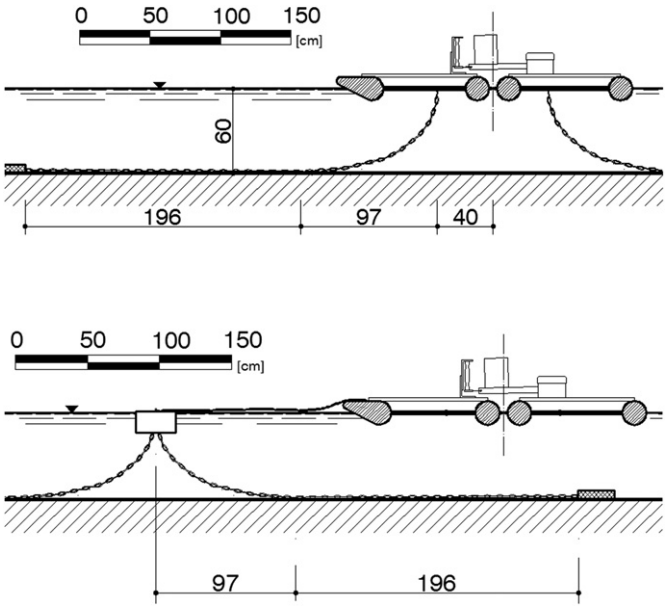

Fig. 4. Cross-shore scheme of DEXA with spread mooring (top) and with CALM system (bottom).

2.3. Tested wave conditions

Wave State (WS) parameters were selected essentially to assess more in depth the dependence of the device performance on the device length to peak wave length ratio l/L_p and also to investigate the effects of wave steepness s_p, i.e. the significant wave height to peak wave length ratio, and wave obliquity β.

WS parameters are reported in Table 1. Each set of WSs was reproduced as irregular 3D short-crested waves with Jonswap spectrum (directional spreading factor of 10). Water depth was kept constant: $h = 0.6$ m. Table 1 also includes a set of equivalent regular WSs adopted to define the best PTO rigidity, as in the usual "Proof of Concept" for testing WECs [7].

These wave attacks were performed under 3 different orientations of the device with respect to the incident wave (always directed perpendicular to the shore): $\beta_1 = 0°$, $\beta_2 = 15°$, $\beta_3 = 30°$, where β is the angle between the device and the basin axis. The different obliquities were obtained by rotating the model, its

Table 1
Irregular and regular tested WSs in 1:30 scale.

Regular WSs					
WS	H_s [m]	T_p [s]	WS	H_s [m]	T_p [s]
1	0.047	1.05	6	0.070	1.94
2	0.047	1.19	7	0.093	1.43
3	0.070	1.05	8	0.093	1.94
4	0.070	1.19	9	0.117	1.43
5	0.070	1.43	10	0.117	1.94
Irregular WSs					
WS	H_s [m]	T_p [s]	WS	H_s [m]	T_p [s]
1	0.067	1.05	6	0.100	1.94
2	0.067	1.19	7	0.133	1.43
3	0.100	1.05	8	0.133	1.94
4	0.100	1.19	9	0.167	1.43
5	0.100	1.43	10	0.167	1.94

Author's personal copy

mooring system and the whole measurement equipment around a reference fixed point in the basin, corresponding to Wave Gauge (WG) nr.3 in Fig. 5.

2.4. Measurements

The hydrodynamic measurements were performed by using in the basin up to 16 resistive Wave Gauges (WGs), which provide the instantaneous value of the surface elevation (Fig. 5). All data were simultaneously acquired at the sample frequency s_f of 20 Hz by means of WaveLab, a software developed by Aalborg University [10].

In presence of both mooring systems, one array of 5 WGs was placed in front of the device to evaluate the incident and reflected waves. For estimating the transmitted wave height, another 5 WGs array was placed behind the device in case of the spread mooring, whereas for the CALM mooring an array of 3 aligned WGs was adopted due to the limited space between the device and the beach. The 5WGs arrays are used to derive the directional wave spectrum by means of the Bayesian Directional Spectrum Estimation Method, BDM, [11]. The method by Mansard and Funke [12] was applied to the 3 WGs array to obtain the significant wave height and peak period, H_s and T_p. In order to derive the changes of the wave field around DEXA, the remaining 6/8 WGs – depending on which spread or CALM system was adopted – were placed along one side of the device.

A force transducer (i.e. a "bone" equipped with strain gauges, to the right of Fig. 3) and an ultrasonic displacement sensor combined with a reflective plate (respectively to the left and to the right of Fig. 3) were used on board of the model to evaluate its power performance.

3. Power performance

3.1. PTO optimisation

The instantaneous values of the produced power are estimated by multiplying forces from the "bone" and velocities from the displacement acquired by the ultrasonic sensor as follows:

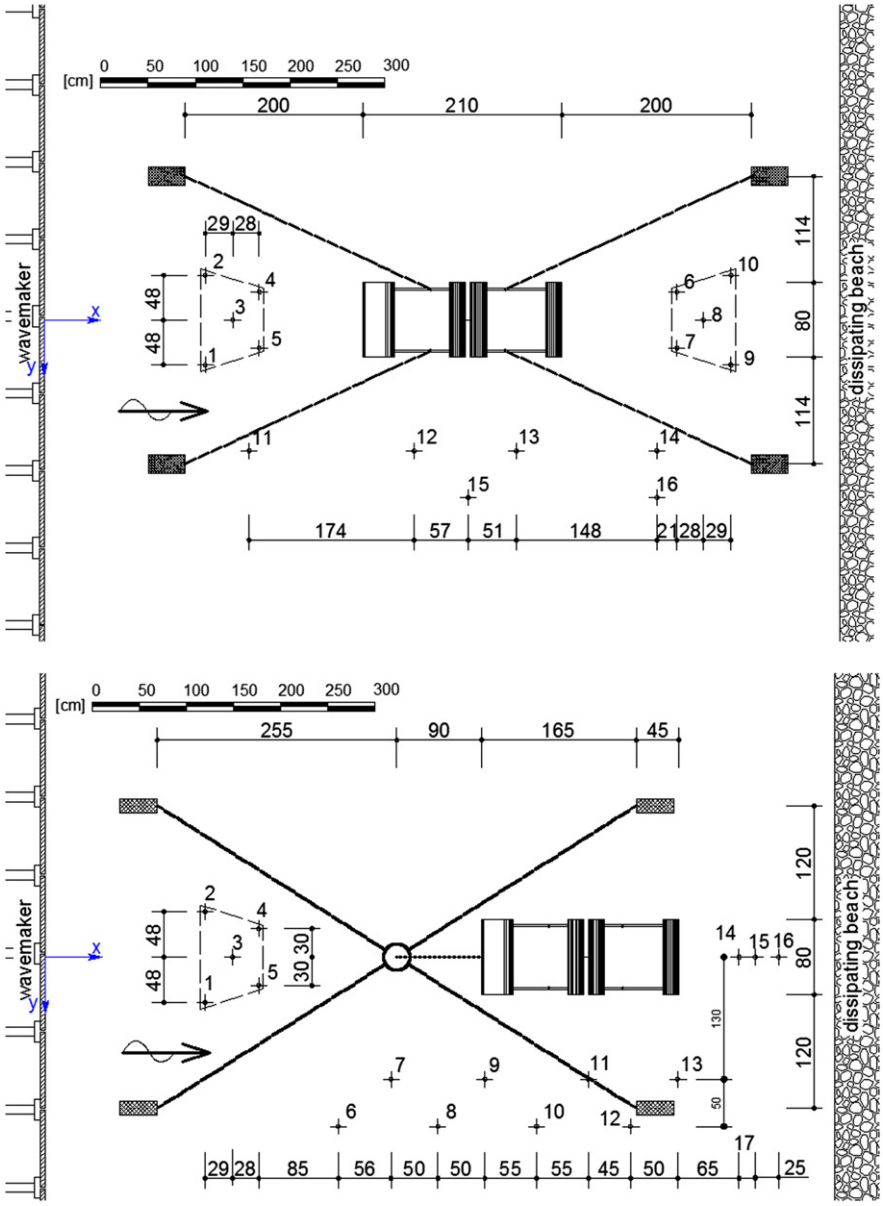

Fig. 5. Plan view of the model with spread (top) and calm (bottom) mooring system. Position of the wave gauges in the basin.

Author's personal copy

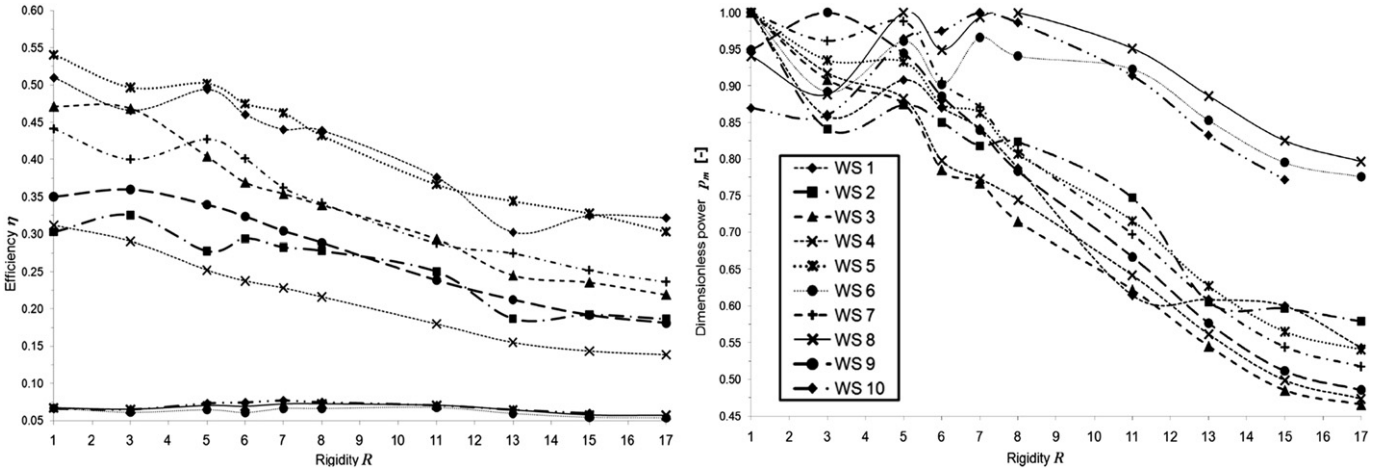

Fig. 6. Efficiency (top) and dimensionless power (bottom) against PTO rigidity for spread mooring.

$$P_m(t) = \left(\frac{F(t)+F(t+\Delta t)}{2}\right)\frac{\mathrm{d}(t+\Delta t)-\mathrm{d}(t)}{\Delta t} \quad (1)$$

where $P_m(t)$ is the instantaneous measured power, F is the force, t is time and the time interval Δt is equal to $1/s_f$. The efficiency η is then computed as the ratio between the average measured power P_m obtained from Eq. (1) and the measured incident wave power per metre crest width P_w multiplied by the device width b:

$$P_W = \frac{\rho g^2 H_s^2 T_{m-1,0}}{64\pi} \quad (2)$$

where $T_{m-1,0}$ is the wave energy period.

The optimisation procedure consisted of two main steps:

- evaluation of P_m and of η for every regular WS, in order to define the optimal PTO rigidity R_{opt} which maximizes both;
- once R_{opt} is defined for every WS, the best PTO rigidity R_B is chosen based on the combination of the best performance at higher and lower WSs (which generally are characterized by different values of R_{opt}) and of the results in terms of P_m and η. The obtained R_B is then used for each corresponding irregular WS.

Within the first step of the procedure, 10 out of the available 17 rigidities were tested with the spread mooring system. Fig. 6 shows the curves representing η and the dimensionless power p_m for each WS versus the rigidity values. The dimensionless power is defined as:

$$p_m = \frac{P_m}{P_M} \quad (3)$$

where P_M is the maximum value of measured power recorded during the test.

Most of the η curves in Fig. 6 have their maxima when $R_{opt} = 1$, 3 or 5, suggesting in particular to consider $R_{opt} = 1$. In this case, however, very large displacements of the metal bar were observed that could lead to non-representative measurements (i.e. displacements out of scale for the measuring system) and damage in time of the whole PTO system (i.e. fatigue effects). In most cases the curves of P_m in Fig. 6 show a well pronounced peak for $R_{opt} = 5$. Therefore based on the combination of these results a constant value of R_B equal to 5 was assumed.

In case of the CALM mooring, Fig. 7 shows that the peak values of η are reached when $R_{opt} = 3$ or 5, whereas P_m is maximum when $R_{opt} = 1$, 3 or 5 for small waves and when $R_{opt} = 5$, 8 and 11 for

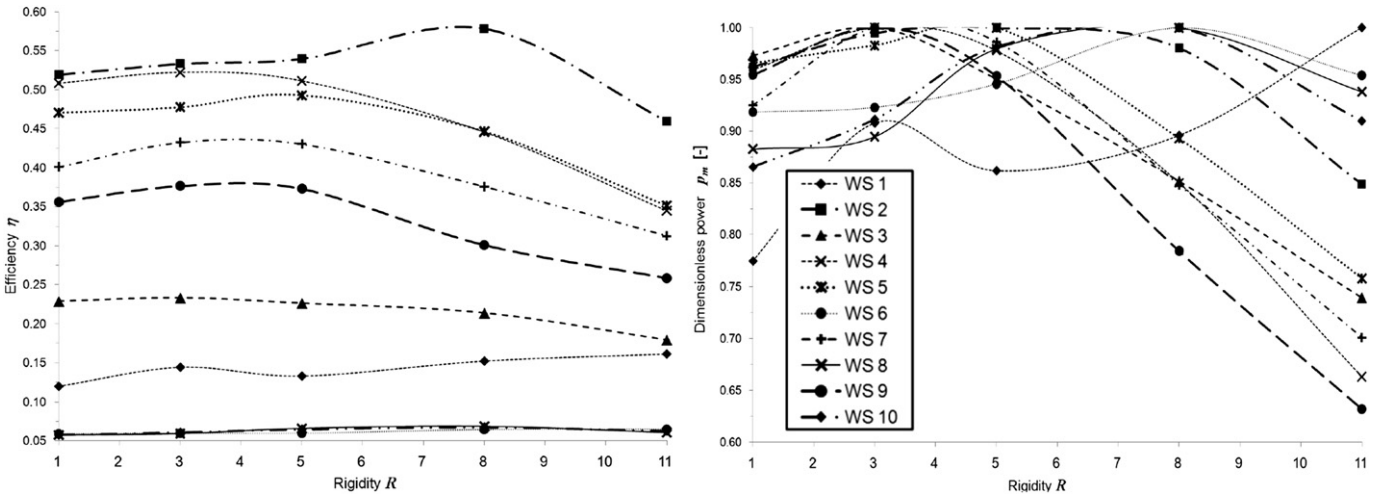

Fig. 7. Efficiency (top) and dimensionless power (bottom) against PTO rigidity for CALM mooring.

Author's personal copy

high waves. As a compromise the value of R_B equal to 5 was again selected.

3.2. Power production

Table 2 synthesises the power production and the efficiency with varying the placement of the device for both mooring systems. The values of P_m and η are significantly greater in case of the CALM than of the spread mooring, with the exception of the greater obliquity β_3. The values of η for spread mooring compared to CALM system are on average 3% lower for β_1, 2% lower for β_2 and 1.4% greater for β_3, whereas the values of P_m differ on average of 31 kW for β_1, 12 kW for β_2 and -19 kW for β_3 (values in full scale).

Fig. 8 shows the dependence of P_m and of η on l/L_p. The sets of P_m tend to decrease with increasing l/L_p, reaching their maxima when l/L_p is around 0.73 for the aligned configuration and 0.76 for the oblique ones. The values of η increase with increasing l/L_p, reaching their maxima when l/L_p is around 1.05.

4. Hydraulic performance

4.1. Wave transmission and reflection

Table 3 synthesises the transmission and reflection coefficients induced by the single device. The transmission coefficient K_T is usually defined as the transmitted to incident significant wave ratio,

$$K_T = \frac{H_T}{H_I} \tag{4}$$

where H_T and H_I are the incident significant wave heights respectively inshore and off-shore the structure or obstacle or device under exam.

Similarly, the reflection coefficient K_R is given by,

$$K_R = \frac{H_R}{H_I} \tag{5}$$

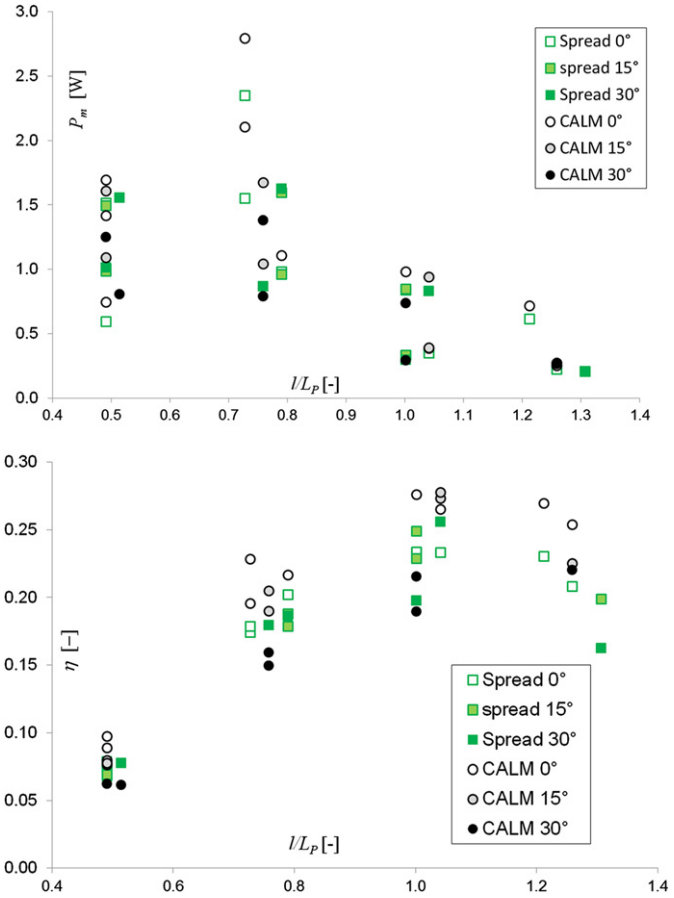

Fig. 8. Power and efficiency η against l/L_p for different obliquities and with two mooring systems.

where H_R is the reflected wave height from a structure or an obstacle or a device.

H_I and H_R are derived from the BDM analysis of the front 5WGs array for spread and CALM system. H_T is derived from the BDM analysis carried out on the back 5WGs array in case of spread

Table 2
Values of η, P_w and P_m for different obliquities and mooring systems.

β_1				β_2				β_3			
WS	P_w [W]	P_m [W]	η [−]	WS	P_w [W]	P_m [W]	η [-]	WS	P_w [W]	P_m [W]	η [−]
Spread mooring system											
1	1.35	0.23	0.21	1	1.30	0.21	0.20	1	1.58	0.21	0.16
2	1.88	0.35	0.23	2	1.85	0.34	0.23	2	1.87	0.30	0.20
3	3.34	0.61	0.23	3				3			
4	4.50	0.84	0.23	4	4.26	0.85	0.25	4	4.05	0.83	0.26
5	6.06	0.98	0.20	5	6.39	0.96	0.19	5	6.06	0.87	0.18
6	10.33	0.59	0.07	6				6			
7	11.14	1.55	0.17	7	11.19	1.60	0.18	7	10.92	1.62	0.19
8	18.44	1.01	0.07	8	17.21	0.98	0.07	8	16.11	1.01	0.08
9	16.47	2.35	0.18	9				9			
10	27.59	1.51	0.07	10	27.20	1.50	0.07	10	25.19	1.56	0.08
CALM system											
1	1.34	0.27	0.25	1	1.39	0.25	0.22	1	1.50	0.26	0.22
2	1.83	0.39	0.26	2	1.80	0.39	0.27	2	1.91	0.29	0.19
3	3.31	0.71	0.27	3				3			
4	4.43	0.98	0.28	4	4.24	0.94	0.28	4	4.28	0.74	0.22
5	6.39	1.11	0.22	5	6.35	1.04	0.20	5	6.21	0.79	0.16
6	10.51	0.75	0.09	6				6			
7	11.51	2.10	0.23	7	11.01	1.67	0.19	7	11.57	1.38	0.15
8	18.24	1.42	0.10	8	17.16	1.09	0.08	8	16.48	0.81	0.06
9	17.88	2.79	0.20	9				9			
10	27.74	1.69	0.08	10	25.98	1.61	0.08	10	25.19	1.25	0.06

Table 3
Values of transmission coefficient K_T, reflection coefficient K_R for different obliquities and mooring systems.

β_1			β_2			β_3		
	K_T	K_R		K_T	K_R		K_T	K_R
1	0.806	0.321	1	0.865	0.308	1	0.936	0.329
2	0.836	0.267	2	0.875	0.258	2	0.940	0.266
3	0.799	0.261	3			3		
4	0.821	0.263	4	0.870	0.265	4	0.937	0.260
5	0.848	0.203	5	0.834	0.201	5	0.873	0.209
6	0.823	0.276	6			6		
7	0.843	0.204	7	0.824	0.204	7	0.893	0.191
8	0.828	0.233	8	0.840	0.241	8	0.874	0.168
9	0.855	0.204	9			9		
10	0.815	0.240	10	0.836	0.243	10	0.869	0.197
1	0.694	0.239	1	0.861	0.253	1	0.910	0.262
2	0.747	0.232	2	0.848	0.228	2	0.837	0.225
3	0.676	0.232	3			3		
4	0.704	0.216	4	0.810	0.228	4	0.849	0.216
5	0.749	0.222	5	0.778	0.217	5	0.792	0.210
6	0.751	0.260	6			6		
7	0.739	0.217	7	0.785	0.212	7	0.786	0.198
8	0.754	0.244	8	0.735	0.211	8	0.726	0.186
9	0.751	0.218	9			9		
10	0.749	0.240	10	0.747	0.198	10	0.742	0.182

Author's personal copy

mooring and from Mansard and Funke's to the 3 WGs back Array for the CALM system.

An important remark is that wave transmission and reflection in presence of an f-WEC of limited dimensions are both dependant on the distance from the device. As already highlighted in the literature on numerical modelling performed of WEC arrays -and also specifically of Dexa [13]- the wave radiated/diffracted by the devices affect the devices placed along the adjacent inshore line and may also lead in turns to modification of the wave field approaching the off-shore line of the wave farm. Therefore the values of K_R and K_T reported here provide only the indication of the magnitude of these process at a fixed location.

Fig. 9 shows the reflection coefficient K_R as a function of l/L_p for the two mooring systems and different obliquities. A great amount of the wave motion is still transmitted behind the device, K_T being always greater than 0.65 (as in preliminary tests, see Ref. [14]). K_T is considerably affected by β and it is found to depend weakly on l/L_p.

The high average value of K_T indeed suggests that there will be enough residual wave energy to allow for the installation of an array of devices inshore this first line to increase power production. Indeed the such high value of K_T suggests also that more cross-shore lines of devices may be necessary to pursue the secondary benefit of reducing the incident wave on the littoral.

The type of the mooring system plays a key role. For the spread mooring, the mean values of K_T are 0.83, 0.84 and 0.88 respectively for β_1, β_2 and β_3. These values are determined within each configuration through a weighted average based on the off-shore incident P_W. When the device is aligned with the incoming waves, K_T increases up to reach its maximum when l/L_p equals 0.73, then it decreases to around 0.80. For oblique conditions, K_T is almost constant with l/L_p. In order to minimize K_T for each WS (also oblique ones), l/L_p should be around 0.75.

K_T decreases with increasing β and therefore wave absorption/dissipation is maximised when the device is placed with a modest obliquity with respect to the incoming waves. The device indeed rotates to align its axis perpendicularly to the incident wave direction, leading to a greater obstacle to the incident waves and therefore a lower amount of transmitted wave motion. Such effect is more appreciable for higher obliquities (β_3), since sway/surge device motions tend to decrease with increasing β.

For oblique conditions, K_T reaches the maximum when l/L_p is around 1.00, and then it tends to a constant value (0.87 for β_2 and 0.94 for β_3).

For the CALM system, the average value of *KT* equals 0.74, 0.76 and 0.86 respectively for β_1, β_2 and β_3. In case of oblique placement of the device, *KT* linearly increases with *l/Lp*, reaching the maximum when $l/Lp = 1.26$ (0.91 for β_2 and 0.86 for β_3). When the device is aligned with the incoming waves, *KT* instead slowly decreases with increasing *l/Lp*. For long waves (i.e. $l/Lp < 0.50$) *KT* is not apparently affected by the obliquity, since all the data provide mostly the same value for *KT*. The explanation of this performance can be found again in the device movements. In all the configurations, the device essentially oscillates around the wave buoy, with larger movements with increasing β and therefore greater residual energy captured by the WG array placed behind the device.

Based on Fig. 10 and on the values given in Table 3, the following results can be derived on wave reflection induced by the device.

K_R increases with increasing the dimensionless model length l/L_p, the trend being similar for aligned and oblique configurations. The increasing rate is lower in case of the CALM system. For perpendicular WSs, the average minimum K_R ($K_R = 0.20$ in case of spread mooring and $K_R = 0.22$ in case of CALM system) is achieved when $l/L_p = 0.76$.

K_R is slightly and not systematically affected by the obliquity: it tends to decrease with increasing β for low values of l/L_p, whereas it tends to increase with increasing β for high values of l/L_p.

K_R depends on the adopted mooring system. In particular, K_R is lower for the CALM system than for the spread mooring. The average values of K_R respectively for β_1, β_2 and β_3 are 0.25, 0.25 and 0.23 in case of the spread mooring and 0.23, 0.22 and 0.21 in case of the CALM mooring.

4.2. Wave field in the wake of the device

In order to describe the wave field in the wake of the device, Fig. 11 shows the values of H_s measured at WGs nr. 7, 8, 14 and 16 against the distance from model axis, for each WS and for each obliquity in the spread mooring system configuration.

For the first four WSs, since the model motion is modest, the values of H_s obtained at the WGs aligned with the device are not affected by the scattered wave field and the highest values of H_s are found at the farthest point of the wake.

For oblique configurations, the model tends to re-orient itself, by aligning its axis along the incoming waves, and radiated waves affect the measurements both at WGs 7 and 14, leading to higher values of H_s.

The wave field in the wake of the device therefore strongly depends on the superposition of heaving motions and device axis reorientation.

It is worthy to note that the device effects in the wake persist for a long-shore distance of about 60 m from the device axis, i.e. 2.5

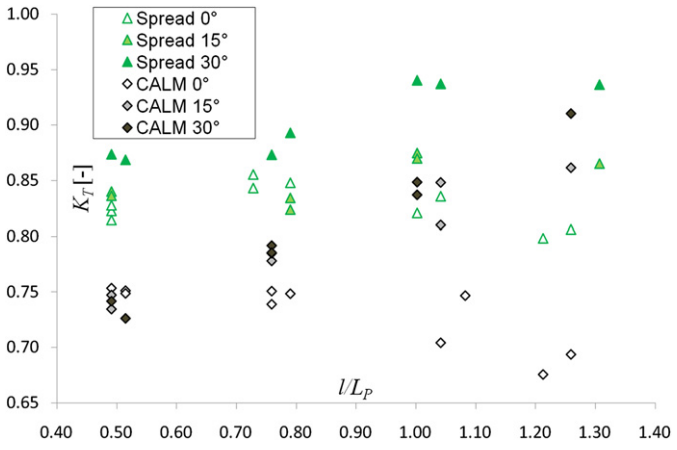

Fig. 9. K_T against l/L_p with spread and CALM mooring system for different obliquities.

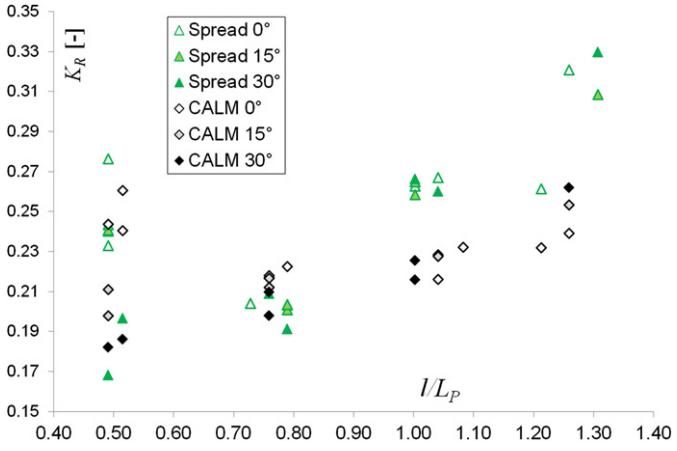

Fig. 10. K_R against l/L_p for different mooring types and different obliquities.

Author's personal copy

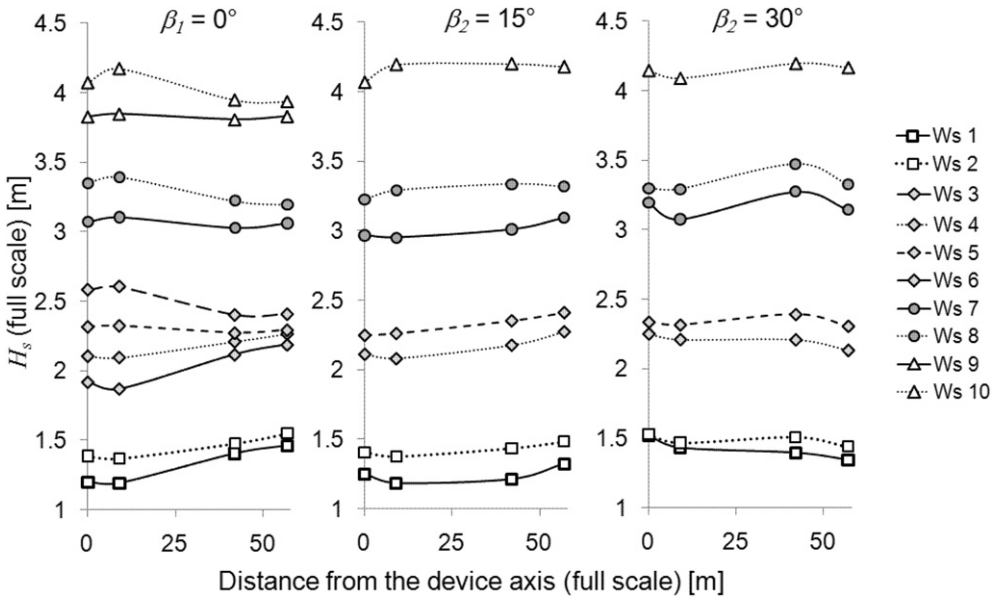

Fig. 11. Wake effects behind the 1:30 scale model. Values of the significant wave height *Hs* measured at WGs nr. 8, 7, 14 and 16 against the distance from model axis, for each WS and for each obliquity.

times the device width. This result is in agreement with previous literature [15–18], investigating the park effect for arrays of WECs characterised by typical dimensions of about 10–20 m. The numerical results of these works showed that the park effect on the device performance becomes hardly noticeable as soon as the distance is larger than about 50–100 m. Thanks to the limited long-shore extension of its wake, also the DEXA device is suitable to be placed in arrays provided that the devices are placed at a mutual long-shore distance –measured as the one between two adjacent devices on two adjacent cross-shore lines- that should be as a minimum equal to around 3 times the width.

4.3. Changes in wave direction

In order to verify the effects on devices placed in a hypothetical inshore line and on sediment transport processes, the changes in wave direction behind the DEXA were evaluated in case of the spread mooring under aligned and oblique configurations. Such variations are represented by means of $\Delta\beta$ that is defined as:

$$\Delta\beta = \beta_I - \beta_T \tag{6}$$

where β_I and of β_T are computed by means of the BDM analysis of the measurements gained from front and back WGs arrays, respectively; therefore, β_I coincides in the different cases with β_1, β_2 and β_3. In all configurations, both WGs arrays were aligned with the device axis.

$\Delta\beta$ is affected by l/L_p, see Fig. 12. The difference in $\Delta\beta$ decreases with increasing l/L_p. When $l/L_p \geq 1.0$, $\Delta\theta$ has the same sign for all the device obliquities.

In most tested conditions, for similar values of l/L_p, the greater the β_I the greater the $\Delta\beta$. This result can be justified by the tendency of the device to re-orient itself perpendicularly to the incident waves, offering a larger surface against them, and to the greater device motion with increasing β and consequent greater delay in its reorientation back to the initial position. This interpretation is confirmed by comparing Fig. 12 with Fig. 9: the larger the $\Delta\beta$ the smaller the *KT*.

The maximum values of $\Delta\beta$ are reached for β_3 and are around $-6°$ and $5°$ when respectively $l/L_p = 0.4$ and $l/L_p = 1.0$.

It is therefore suggested to place the device aligned with the main incident wave direction, in order to minimize the changes of the transmitted wave direction and thus to minimise -at local scale- possible uncontrolled effects on other devices placed in the same farm and -at large scale- changes in sediment transport patterns.

4.4. Device optmisation

In the perspective of integrating DEXA in a multi-purpose marine farm, the results of wave transmission and of power performance are synthesised and examined.

The sets of η and of K_T, together with their second order tendency curves, are plotted and compared in Fig. 13. The curve coefficients are computed by means of the ordinary least squares method.

The CALM system always provides better results than the spread mooring in terms of wave absorption/dissipation (lower K_T) and energy production (greater η).

K_T decreases with increasing l/L_p when the device is aligned with the incoming waves, whereas it linearly increases with increasing l/L_p in oblique configurations. In all tested conditions,

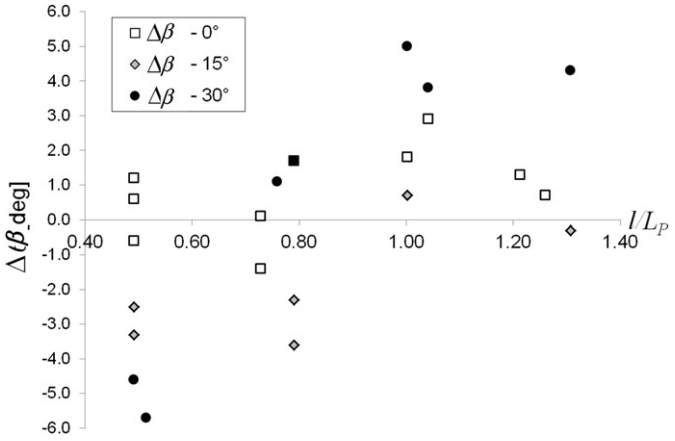

Fig. 12. Difference between incident and transmitted wave direction $\Delta\beta$ against l/L_p. Spread mooring system.

Author's personal copy

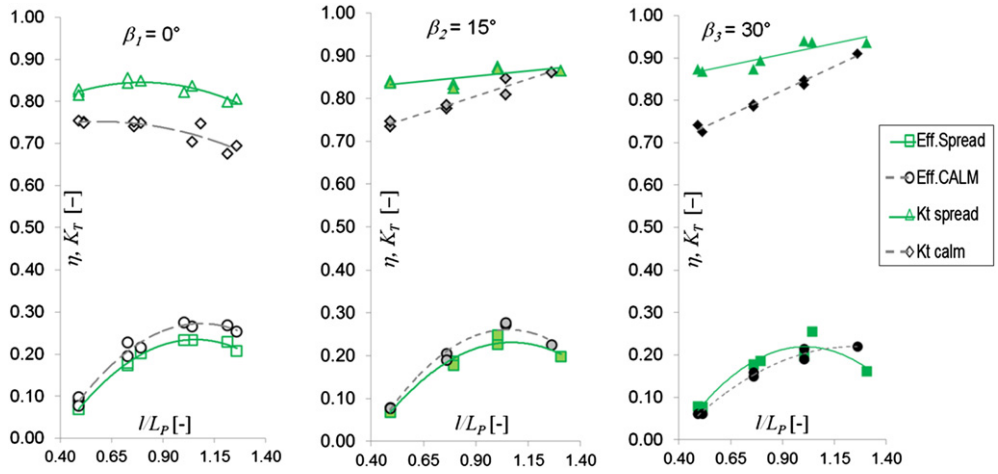

Fig. 13. Comparison among η and K_T curves for different obliquities and mooring systems.

η has a peak when l/L_p is about 1.0 then it tends to decrease more markedly for oblique placements of the device. Therefore – based on the combined results of K_T and η for β_1 and based on the results of η only for β_2 and β_3 – a reasonable choice is to identify $l/L_p \sim 1.0$ as the optimal design value.

5. Conclusions

Tests were carried out in the Aalborg wave basin to jointly examine the hydrodynamics and the power production of a single Wave Activated Body device, called DEXA, reproduced in 1:30 scale.

Experimental results show that the device length l has to be 'tuned' on the basis on the local peak wave length (i.e., the more frequent wave length within the typical yearly climate) and specifically the condition $l/L_p = 1.0$ has to be assured for most of the year since it leads to the best compromise between power production performance and wave transmission, regardless of he mooring system is adopted.

The CALM mooring system leads always to a larger power production than a spread mooring, especially when wave direction is aligned with the device axis; limitedly to this case, it also induce a higher wave absorption.

The device should be placed with the axis oriented along the local dominant direction of incoming waves in order to maximise wave absorption. Residual wave energy however is always rather high, being $K_T > 0.65$, and therefore should be captured by other devices placed along inshore lines within the same array.

The device induces a change in wave direction $\Delta\beta$ of few degrees that should be carefully accounted for when examining the effects such installation may produce on other devices in the same array or on near-shore sediment transport processes. Also the values of $\Delta\beta$ show a slight dependence on l/L_p: the greater the l/L_p, the smaller the differences of $\Delta\beta$.

Acknowledgements

The support of the European Commission through FP7.2009-1, Contract 244104 – THESEUS project ("Innovative technologies for safer European coasts in a changing climate"), www.theseusproject.eu, and the support of the Danish Council for Strategic Research through SDWED project (Structural Design of Wave Energy Devices), www.sdwed.civil.aau.dk, are gratefully acknowledged.

The authors wish to acknowledge Lars Clausen, DEXA energy, for providing the small scale devices, and Niels Drustrup, technician at Aalborg University, for the great support during the tests.

References

[1] Harris RE, Johanning L, Wolfram J. Mooring systems for wave energy converters: a review of design issues and choices. In: Proceedings of international conference on marine renewable energy, Blyth, UK; 2004.
[2] Vicente PC, Falcão AFO, Justino PAP. Non-linear slack-mooring modelling of a floating two-body wave energy converter. In: Proc. Ewtec 2011-9th European wave and tidal energy conference, Southampton; 2011.
[3] Nørgaard JH, Poulsen M. Wave height reduction by means of wave energy converters. MSc in Civil Engineering, 4th. Semester, Aalborg University, http://mhk.pnnl.gov/wiki/images/3/3c/Norgaard_%26_Poulsen_2010.pdf; 2010.
[4] Hales LZ. Floating breakwaters: state-of-the-art literature review. US Army Coastal Engineering Research Center; 1981. CERC-TR-81-1.
[5] Martinelli L, Ruol P, Zanuttigh B. Wave basin experiments on floating breakwaters with different layouts. Applied Ocean Research 2008;30:199–207.
[6] Giles ML, Sorensen RM. Determination of mooring loads and transmission for a floating tire breakwater. In: Proc. Coastal Structures, vol. II. ASCE; 1979. p. 1069–86.
[7] Kofoed JP. Hydraulic evaluation of the DEXA wave energy converter. DCE contract report No. 57. Dep. of Civil Eng. Aalborg University; 2009.
[8] Aalborg University. AwaSys homepage. http://hydrosoft.civil.aau.dk/AwaSys, (2007a).
[9] Esmailzadeh E, Goodarzi A. Stability analysis of a CALM floating off-shore structure. International Journal of Non-Linear Mechanics 2001;36:917–26.
[10] Aalborg University. WaveLab 2 homepage. http://www.hydrosoft.civil.auc.dk/wavelab (2007b).
[11] Hashimoto N, Kobune K. Estimation of directional spectrum from a Bayesian approach. In: Proc.21st international conference on coastal engineering, vol. 1. ASCE; 1988. p. 62–72.
[12] Mansard EPD, Funke ER. The measurement of incident and reflected spectra using a least squares method. In: Proc. 17th Int. Conf. Coastal Eng. New York: ASCE; 1980. p. 154–72.
[13] Zanuttigh B, Angelelli E. Experimental investigation of floating wave energy converters for coastal protection purpose. Coastal Engineering, in press. http://dx.doi.org/10.1016/j.coastaleng.2012.11.007.
[14] Zanuttigh B, Martinelli L, Castagnetti M, Ruol P, Kofoed JP, Frigaard P. Integration of wave energy converters into coastal protection schemes. In: Proc. 3rd international conference on ocean energy (ICOE), Bilbao; 2010.
[15] Ricci P, Saulnier JB, Falcão AFO. Point-absorber arrays: a configuration study off the Portuguese West-Coast. In: Proc., of the 7th European wave and tidal energy conference, Porto, Portugal; 2007.
[16] Cruz J, Sykes R, Siddorn P, Eatock Taylor R. Wave farm design: preliminary studies on the influences of wave climate, array layout and farm control. In: Proc. of the 8th European wave and tidal energy conference. Uppsala: Sweden; 2009.
[17] Babarit, impact of long separating distances on the energy production of two interacting wave energy converters. Ocean Engineering 2010;37:718–29.
[18] Borgarino A, Babarit P. Ferrant, Impact of wave interactions effect on energy absorption in large arrays of wave energy converters. Ocean Engineering 2011;41:79–88.

Glossary

b: model width
c_I: ratio between H_I at different scales
c_R: ratio between H_R at different scales
c_T: ratio between H_T at different scales

Author's personal copy

d: PTO displacement
F: PTO force
h: water depth
H_I: incident wave height
H_R: reflected wave height
H_s: significant wave height (time domain)
H_T: transmitted wave height
K_D: dissipation coefficient
K_R: reflection coefficient
K_T: transmission coefficient
l: model length
l/L_p: dimensionless model length
L_p: peak wave length
P_m: produced mechanical power
P_M: maximum produced power of a single wave state
p_m: dimensionless power
P_w: incident wave power
R: PTO rigidity
R_B: best PTO rigidity accounting for all the wave states
R_{opt}: optimal PTO rigidity for a single regular wave state
s_f: sample frequency (20 Hz)
s_p: peak wave steepness
t: time
T_p: peak period
β: orientation of the device axis with respect to incoming waves perpendicular to the shore
$\Delta\beta$: difference between the incident and transmitted wave directions
η: efficiency of the device